

A Review of Deep Learning Approaches for Inverse Scattering Problems

Xudong Chen^{1, *}, Zhun Wei², Maokun Li³, and Paolo Rocca^{4, 5}

(Invited Review)

Abstract—In recent years, deep learning (DL) is becoming an increasingly important tool for solving inverse scattering problems (ISPs). This paper reviews methods, promises, and pitfalls of deep learning as applied to ISPs. More specifically, we review several state-of-the-art methods of solving ISPs with DL, and we also offer some insights on how to combine neural networks with the knowledge of the underlying physics as well as traditional non-learning techniques. Despite the successes, DL also has its own challenges and limitations in solving ISPs. These fundamental questions are discussed, and possible suitable future research directions and countermeasures will be suggested.

1. INTRODUCTION

Deep learning (DL) has recently shown outstanding performance on object classification and segmentation tasks in computer vision [1]. Motivated by these successes, researchers have begun to apply DL to several research fields including inverse problems. The purpose of this paper is to summarize recent works using DL for inverse scattering problems (ISPs). ISPs are concerned with determining the nature of an unknown scattering distribution (e.g., the shape, the position, and the material properties), from the knowledge (measure) of the scattered fields. Using electromagnetic or acoustic waves to probe obscured or remote regions, the imaging techniques based on ISPs are suitable for a wide range of important applications, such as remote sensing, nondestructive evaluation, geophysics, security check, biomedical imaging and diagnosis, and through-wall imaging. Since ISPs generally involve reconstructing the values of physical parameters (such as permittivity) of scatterers, it is also referred to as quantitative imaging. ISPs are challenging to solve because they are intrinsically ill-posed and nonlinear. This paper focuses on solving full-wave non-linear ISPs by taking into account multiple scattering phenomena.

ISPs can be tackled by either traditional objective-function approaches or learning approaches. The former ones easily incorporate domain knowledge (i.e., wave physics for ISPs) into its model, but they are usually computationally expensive due to the iterative nature. Otherwise, learning techniques provide a solution in real time, but it is not easy to incorporate domain knowledge. Naturally, how to bridge the gap between objective-function approaches and machine-learning based techniques forms a fertile ground for future investigations of the whole ISP community. Indeed, for many engineering and physical problems, researchers have gained, over several decades, much insightful domain knowledge that

Received 7 March 2020, Accepted 23 June 2020, Scheduled 29 June 2020

* Corresponding author: Xudong Chen (elechenx@nus.edu.sg).

¹ Department of Electrical and Computer Engineering, National University of Singapore, Singapore 117583, Singapore. ² Key Lab. of Advanced Micro/Nano Electronic Devices & Smart Systems of Zhejiang, College of Information Science and Electronic Engineering, Zhejiang University, Hangzhou 310027, China. ³ Beijing National Research Center for Information Science and Technology (BNRist), Department of Electronic Engineering, Tsinghua University, Beijing 10084, China. ⁴ ELEDIA@UniTN (DISI — University of Trento), Trento 38123, Italy. ⁵ ELEDIA Research Center (ELEDIA@XIDIAN — Xidian University), Xi'an 710071, China.

has been leveraged on to devise approximate direct inversion models or effective iterative solvers. Thus, to avoid using DL as a purely data-driven black-box solver, it is of paramount importance to address the problem of how profitably combining DL with the available knowledge on underlying physics as well as traditional objective-function approaches. Many research efforts have been made in this direction to achieve real-time quantitative imaging.

This paper discusses DL from the perspective of drawing insights from physics, which helps to avoid a brute-force (or black-box) way of using DL. This perspective is different from other perspectives. For example, [2] and [3] design neural networks (NNs) inspired by optimization algorithms, where iterative optimization algorithms are unrolled and then each iteration is turned into a layer of a network. In [4], many existing effective networks are interpreted as different numerical discretizations of differential equations, [5] finds that there is a close connection between discrete dynamic systems and deep networks with skip connections, and [6] establishes a mathematical foundation for investigating the algorithmic and theoretical links between optimal control and DL. In contrast to the aforementioned perspectives, the physical perspective deploys existing DL networks to solve an equivalent but less challenging problem, such as mapping reformulated inputs to outputs, which is carefully stated by incorporating domain knowledge into DL network. The physical-insight perspective applies not only to ISPs, but also to many other physical regression problems. Indeed, in many real-world applications, data collected by sensors (e.g., optical wave, acoustic wave, microwave wave, electric current/voltage, heat, etc.) are automatically governed by physical laws. Some of these physical laws present well-known mathematical properties (even analytical formulas in some cases), which do not need to be learnt by training with a lot of data. We mention in passing that it is not the purpose of this paper to design a more powerful DL network to solve a general regression problem.

More specifically, this paper reviews methods, promises, and pitfalls of DL as applied to ISPs. We introduce several state-of-the-art methods of solving ISPs with DL, and also offer some insights about how to combine NNs with knowledge of the underlying physics as well as traditional non-learning techniques. Despite the successes, DL also has its own challenges and limitations in solving ISPs. We will discuss these fundamental questions and suggest possible suitable future research directions and countermeasures. We assume that readers are equipped with certain knowledge of DL and this paper will not introduce DL itself in great detail since many references are available (see [7] and the references therein). Moreover, readers are required to have the knowledge of forward problem solvers, but not necessarily in-depth understanding of inverse problems.

2. FORWARD AND INVERSE SCATTERING

The research into an inverse problem requires a deep or fairly good understanding of the corresponding forward problem, regardless whether traditional objective-function approaches or learning approaches are adopted. This section formulates the forward and inverse scattering problems, followed by discussing their underlying physical principles.

Figure 1 shows a schematic diagram of a scattering problem. A scatterer is located in the domain D , referred to as the domain of interest (DOI), and it is illuminated by incoming waves generated by transmitters. In the forward problem, the properties of the scatterer are known, and the goal is to calculate the scattered fields that are measured at an array of receivers located at a surface S . As to the inverse problem, for each illumination, the scattered fields are measured at receivers and the goal is to determine the shape, position, and material of the scatterer from the measured scattered fields.

We consider a two-dimensional (2D) scalar wave scattering problem. In a homogeneous medium background that has permittivity ϵ_0 and permeability μ_0 , nonmagnetic dielectric scatterers are located in D and are illuminated by time-harmonic electromagnetic waves. Adopting the time convention $e^{-i\omega t}$, we formulate the forward problem as the following source-type integral equations [8],

$$E^t(\mathbf{r}) = E^i(\mathbf{r}) + k_0^2 \int_D g(\mathbf{r}, \mathbf{r}') J(\mathbf{r}') d\mathbf{r}' \quad \text{for } \mathbf{r} \in D, \quad (1)$$

and

$$E^s(\mathbf{r}) = k_0^2 \int_D g(\mathbf{r}, \mathbf{r}') J(\mathbf{r}') d\mathbf{r}' \quad \text{for } \mathbf{r} \in S, \quad (2)$$

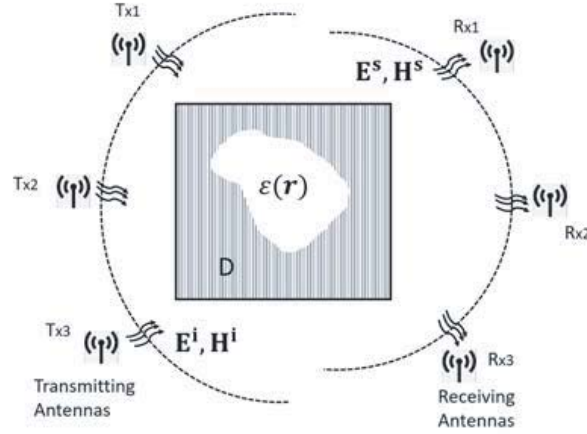


Figure 1. Schematic diagram of the forward and inverse scattering problems.

where $J(\mathbf{r}) = (\epsilon_r(\mathbf{r}) - 1)E^t(\mathbf{r})$ is a normalized contrast current density, and $k_0 = \omega\sqrt{\mu_0\epsilon_0}$ is the wavenumber of the background medium. $\epsilon_r(\mathbf{r}) - 1$ is referred to as the contrast and is denoted as $\chi(\mathbf{r})$. Equations (1) and (2) can be written in a compact form,

$$J(\mathbf{r}) = \chi(\mathbf{r}) [E^i(\mathbf{r}) + G_D(J)] \quad \text{for } \mathbf{r} \in D, \quad (3)$$

$$E^s(\mathbf{r}) = G_S(J) \quad \text{for } \mathbf{r} \in S, \quad (4)$$

which are referred to as the state equation and data equation, respectively.

Physically, the scattering process involves three steps: First, incidence, where some external sources generate an incident wave to illuminate the scatterer; Second, wave-matter interaction, where contrast current is induced in response to the incident field; Third, reradiation, where induced contrast current radiates as a passive source, also known as a secondary source, to generate scattered fields that are collected at receivers. It is clear that the first step involves $E^i(\mathbf{r})$, which is independent of the contrast $\chi(\mathbf{r})$. The second step depends on $\chi(\mathbf{r})$, as shown in Eq. (3). Nevertheless, the operator G_D itself is independent of $\chi(\mathbf{r})$. The third step involves the radiation operator G_S , which is independent of $\chi(\mathbf{r})$. The above analysis shows that $E^i(\mathbf{r})$, G_S , and G_D are independent of the contrast $\chi(\mathbf{r})$, which is the unknown parameter to be recovered in ISPs. Thus, when we apply DL to solve ISPs, it is of paramount importance to fully exploit the domain knowledge provided in the first ($E^i(\mathbf{r})$) and third (G_S) steps, as well as partially in the second step (G_D).

3. OBJECTIVE-FUNCTION AND LEARNING APPROACHES

To present objective-function and learning approaches for solving ISPs, it is more convenient to present them for solving more general inverse problems. Suppose that we want to determine the model parameters, denoted as x , that produce the data y that is the observation we have recorded. Inverse problems consist of looking for the model parameters x such that $y = f(x)$, where f is the forward map. The space of model parameters is denoted by \mathcal{X} and the space of data is denoted by \mathcal{Y} .

3.1. The Two Approaches

The objective function approach, also known as model-based approach, fully exploits the forward model f and recovers an estimate of x from y by solving a minimization problem,

$$f_{obj}^{-1}(y) := \underset{x}{\operatorname{argmin}} \{ \operatorname{mis}\{f(x), y\} + R(x) \}, \quad (5)$$

where $\operatorname{mis}: \mathcal{Y} \times \mathcal{Y} \rightarrow R^+$ is an appropriate measure of mismatch in the data domain, and $R: \mathcal{X} \rightarrow R^+$ is a regularization functional that incorporates our prior knowledge of x . For a nonlinear inverse problem, Eq. (5) is usually solved by iterative methods, and in some cases it can be converted to an approximate

direct inversion model. The minimizer of Eq. (5) is the solution provided by the objective function approach.

The learning approach, also known as data-driven approach, solves inverse problems by processing large amount of available data, without exploiting the corresponding forward mapping. The learning approach for inverse problems usually falls into the category of supervised learning, where a training set of ground-truth model parameters and their corresponding measurements, $\{(x_n, y_n)\}$, $n = 1, 2, \dots, N$, is known. A learning architecture F_θ is first selected, which is equipped with a set of tunable parameters θ in the space of Θ (i.e., $\theta \in \Theta$). The implementation of learning approach consists of the training stage and the testing stage. In the training stage, the parameters θ are ‘‘learnt’’ by solving a regression problem,

$$f_{learn}^{-1}(y) := F_\theta(y), \text{ with } \theta \text{ being } \underset{\theta}{\operatorname{argmin}} \sum_{n=1}^N \operatorname{mis}\{F_\theta(y_n), x_n\} + R(\theta), \quad (6)$$

where $\operatorname{mis}: \mathcal{X} \times \mathcal{X} \rightarrow R^+$ is an appropriate measure of mismatch in the space of model parameter and $R: \Theta \rightarrow R^+$ is a regularization functional to avoid overfitting. In practice, mis is usually chosen as pixel-wise mean squared error (MSE). The minimizer of Eq. (6) finalizes the neural network F_θ , which is then used in the testing stage to quickly generate the prediction $F_\theta(y)$ as the final result provided by the learning approach.

Some comments on the aforementioned two approaches are made as follows:

First, for a nonlinear inverse problem, the objective function approach usually minimizes Eq. (5) in an iterative manner. The so-obtained output x can be interpreted as an implicit inverse $f^{-1}(y)$ of the original forward operator f . In comparison, the learning approach can be interpreted as an approximate explicit inverse of f , where the parameters contained in the formula of the explicit inverse are obtained by fitting large amount of training data.

Second, the learning approach shifts the computational burden to the learning stage whereas the testing stage is computationally efficient. In comparison, the objective function approach relies on optimization algorithms, which solve problems iteratively and are computationally demanding.

Third, it is straightforward for the objective function approach to incorporate prior or domain knowledge into the solution of an inverse problem, whereas it is generally hard to explicitly incorporate such domain knowledge into a learning architecture.

Fourth, in light of the second and third points, how to bridge the gap between objective-function approach and machine-learning approach forms a fertile ground for future investigation. It is important to solve the question of how best to combine NNs with domain knowledge as well as direct and iterative inversion techniques, with the purpose of reducing or relieving the burden on the NNs to learn the well-known physics of the forward model.

Fifth, there is not a strict borderline between the two approaches. In fact, from the mathematical point of view, the objective function formulation (5) can be treated as a special case of the learning formulation (6), where the size of training data N is zero, $\theta = x$, and $R(\theta) = \operatorname{mis}\{f(x), y\} + R(x)$.

3.2. Deep Learning Architectures

A DL neural network consists of a stack of layers, each of which transforms its input to a new representation that is then used as input to the next layers. Each layer is composed of multiple neurons. There is a vast variety of network architectures, such as fully connected neural network, also referred to as the multilayer perceptron (MLP), convolutional neural network (CNN) (including many variants, such as the U-Net, which is an encoder-decoder CNN with skip connections), recurrent neural network (RNN), generative adversarial network (GAN), long-short term memory network (LSTM).

In solving ISPs, most commonly adopted learning architectures are CNN and MLP. These two types of architectures share two similarities. First, the outputs of neurons in one layer are linearly fed to the neurons of the next layers via weights and biases, which are the parameters θ presented in Eq. (6). Second, the linearly transformed input into each neuron undergoes an element-wise nonlinear operations, which is referred to as the activation function, an example of which is the ReLU (Rectified Linear Unit). The key difference between MLP and CNN lies in how the neurons in a layer are connected to the neurons in the next layer. In MLP, each neuron in a layer is connected to all neurons in the next

layer. In comparison, the layer-to-layer connection in CNN is by convolution, which is a local operation. Although theoretically MLP is able to approximate any continuous functions arbitrarily well, it is not suitable to large scale problems due to exceedingly large amount of parameters as a consequence of full connection between layers. In contrast, CNN has much fewer parameters and is more suitable for large scale problems, in particular in dealing with images and videos.

Many aspects of DL architecture are out of the scope of this paper, such as how to choose the number of layers, as well as the number of neurons in each layer, what filter sizes are typically used, how many training data are sufficient, how to obtain training data, how to increase the training set size, and why the stochastic gradient descent (SGD) is popular in minimizing the cost function. Interested readers are referred to [7, 9, 10] and the references therein.

Learning approaches have not yet had the profound impact on inverse problems as they have had for object classification [9]. When we solve ISPs, which are a regression task, special caution must be taken when choosing DL architectures. Architectural choices that work well for a classifier task might be ineffective for solving a regression task.

4. DL APPROACHES FOR ISPS

Although the development of regression techniques based on DL is at the beginning, many research works have been recently carried out in solving ISPs. This review article focuses on DL inversion algorithms for solving ISPs, but it is worth quickly reviewing how early-stage neural networks, which are referred to as shallow NNs in [11], are deployed for such a task.

The early attempts to solve ISPs with shallow NNs have been concerned with the parametric inversion of scatterers. The parameters are of small-size, such as positions, geometries, and homogeneous dielectric properties, mainly due to the limited layer in NN architectures. The training data set consists of scattered field information as the input of network and the ground-truth scatterer as the output. Although it costs plenty of time for NN in the training stage, the trained network is able to solve typical ISPs in real time.

The fully connected NN with one hidden layer is applied in [12] to the detection of cylindric objects inside a given domain of interest, retrieving their geometric and electrical characteristics. The radial basis function neural networks (RBFNNs), with a Gaussian kernel, are adopted in [13] to solve an ISP-formulated microwave medical imaging problem, i.e., to estimate the position and the size of proliferated marrow inside the bone of a limp. The problem of buried object detection is recast into a regression estimation one and successively solved by means of a support vector machine (SVM) in [14]. A support vector regression (SVR) algorithm is performed in [15] to achieve real-time retrieval of the characteristics of a defect with eddy current testing in a nondestructive testing framework.

Thanks to the rapid evolution in the field of artificial intelligence, NNs have evolved into the stage of DL, where much deeper and consequently more powerful networks are used. With DL, a more versatile pixel-based learning approach for inverse problems becomes possible, where unknowns are represented by pixel basis instead of by a few parameters. To apply DLs to solve ISPs is an attractive and fast-developing research area, since real-time quantitative imaging is desirable in many real-world applications. Roughly speaking, DL approaches for such a task can be categorized into four types.

4.1. Direct Learning Approach

The first type is a direct learning approach that directly reconstructs the contrast of scatterer from measurement of scattered field. This type of learning method has to spend unnecessary computational cost to learn well-known wave physics and thus it is able to reconstruct only very simple scatterers. This approach, also referred to as the fully learned reconstruction, works basically as a black box. While the effort required from DL users is minimum, the task for NN itself is heavy.

CNNs are directly applied in [16] to the diagnostic of a dielectric micro-structure, which consists of a finite number of circular cylinders with a fraction of wavelength radius that are set parallel to and at sub-wavelength distance from one another. The aim is to characterize this micro-structure, like positions of rods or their absence, and in effect to map their dielectric contrasts. In [17], parameters of dielectric cylinders, including coordinates of the cylinder center, its radius and the dielectric properties,

are directly estimated from the magnitude of total field by using both MLP and CNN. In [18], for the purpose of comparing with physics-assisted learning approach, a direct inversion scheme (DIS) is performed. In [19], a two-step machine learning approach is proposed. The first step employs original scattered fields as the input and the ground-truth contrast of scatterer as the output. In the second step, the previously obtained contrasts are fed as input into a complex-valued deep residual CNN to refine the reconstruction of images.

The last paragraph of Section 2 suggests that an effective DL algorithm should fully exploit the domain knowledge provided in the first ($E^i(\mathbf{r})$) and third (G_S) steps, as well as partially in the second step (G_D). However, it is clear that direct learning approaches use none of them. Physically, NNs have to implicitly learn the positions of receivers as well as the spatial distribution of incidence fields, both of which are however known parameters.

4.2. Learning-Assisted Objective-Function Approach

The second type still solves ISPs in the framework of traditional objective function approach but employs NNs to learn some components of iterative solvers. This design combines many of good aspects of both the objective-function and learning-based approaches.

The supervised descent method (SDM) is applied in [20] to tackle microwave imaging, which updates the inversion models using the descent directions collected from the training stage. The whole inversion process is divided into two stages: offline training and online prediction. In the first stage, it learns the average descent directions from a training set. In the second stage, unknown parameters can be updated through the pre-learned descent directions together with the data misfit. Because the training set is generated according to prior information, this scheme enables us to incorporate prior information in a more flexible manner. Since this method does not require computing partial derivatives, the computational cost is reduced. Mathematical perspectives of learning gradient are presented in [21].

Another strategy is to apply DL to generate good initial guesses for existing ISP inversion models. In [22], a CNN is designed and trained to learn the complex mapping function from magnetic resonance (MR) T1 images to dielectric images. The predicted dielectric images by the CNN are then used as the starting image for the microwave inverse scattering imaging as a physics-based image refinement step. In [23], a CNN, named CS-Net, is first proposed to be trained to predict a good estimate of the total contrast source, i.e., the $J(\mathbf{r})$ in Eqs. (3) and (4). Then, an existing iterative optimization procedure refines the contrast source estimate obtained at the output of CS-Net. It is important to highlight that the input and output of the CS-Net are the contrast source $J(\mathbf{r})$, instead of the original target parameter, the contrast $\chi(\mathbf{r})$. The input is chosen as the signal-subspace component of the total contrast source, motivated by the subspace-based optimization method (SOM) [24]. The output of CS-Net is the total contrast source. This CNN in fact implicitly learns the noise-subspace components of the radiation operator. The combination of the strengths of both objective-function and learning-based approaches enable this algorithm to recover high permittivity scatterers, i.e., able to tackle more challenging nonlinear problems.

Since the aforementioned methods eventually solve ISPs by objective-function approaches, the requirement on the learning effect of NNs is naturally not stringent.

4.3. Physics-Assisted Learning Approach

The third type solves ISPs using NNs by incorporating domain knowledge together with its mathematical implementation into either the input of NNs or internal architecture of NNs.

Many efforts have been made in deploying domain knowledge to generate an approximate inverse (such as back-propagation), i.e., a reasonably good estimate of the contrast, and then the estimated contrast and ground-truth contrast are chosen as the input-output pair of NNs. Thus, the learning process is simplified by transferring the inputs of NNs from the measurement domain to the contrast domain. Since the estimated contrast that is the input of NNs is a kind of low-resolution version of the ground-truth contrast that is the output of NNs, vastly-available existing NN techniques for image processing that have accumulated in past decades can be directly used. For example, the U-Net CNN inserts a skip connection from the input of the NN to its output layer. This feature is particularly well suited to image restoration problems, when the input and output images share very similar contents.

The U-Net learns to predict the missing high-frequency components from the low-resolution image instead of an entire new mapping function from the low-resolution to the high-resolution image. That is why the U-Net architecture is widely used in solving ISPs. In the U-Net architecture of [25], the input consists of two channels for the real and imaginary parts of the back propagated (BP) low-resolution estimation. The output is a single image of the scattering potential (which is equivalent to the contrast, up to a constant factor). The BP scheme (BPS) presented in [18] also adopts the U-Net, with BP estimation as the input. In [26], the connection (or analogy) between conventional iterative inverse-scattering algorithms and DNNs has been profitably investigated to develop the “deepNIS” DL network, which is based on three cascaded CNNs that process a BP-generated image to determine a fine-resolution guess of the dielectric distribution. The performance of DeepNIS is further evaluated in [27] by several proof-of-concept numerical and experimental demonstrations. In [28], a three-dimensional (3D) electromagnetic ISP with layered media background is solved by using a 3D U-Net, where the input is generated in a two-step procedure: the Born approximation (BA) inversion first yields the preliminary 3D model parameter distribution that is further refined by the Monte Carlo method (MCM). In [29], the input to CNN is the image of the complex tissue permittivity obtained by the contrast source inversion (CSI) [30], a popular iterative objective-function approach solver of ISPs, whereas the CSI has utilized ultrasound-derived tissue regions as prior information. The dominant current scheme (DCS) presented in [18] yields a better estimate of the contrast than the BPS does, using the concept of dominant contrast current. The U-Net is used to learn the difference between the input contrast and the output contrast.

Physical knowledge and its mathematical properties can also be exploited to design desirable architecture of NNs. In [31], the NN still provides a map between the scatterers and the scattered field, but it introduces a novel switching layer with sparse connections. The new NN architecture, named the SwitchNet, uses far fewer parameters and facilitates the training process. The model is motivated by the Born approximation and is designed for far-field placement of transmitters and receivers. The paper carefully analyzes the inherent low-rank structure of the scattering problems, which motivates the introduction of a novel switching layer with sparse connections. It is pointed in [31] that if a NN still provides a map between the scatterers and the scattered field, then a typical CNN with local connections is usually inapplicable since a scatterer has a global impact on the scattered wave field.

For physics-assisted learning approaches, the properties of $E^i(\mathbf{r})$, G_S , and G_D have been used, to a certain degree, to generate the input to NNs or to design internal architecture of NNs.

4.4. Other Approaches

In [32], an induced current learning method (ICLM) is designed, which consists of several strategies to incorporate physical expertise inspired by traditional iterative algorithms into the NN architecture. Inspired by contrast-source type iterative inversion solvers, it reformulates the problem to estimating contrast current $J(\mathbf{r})$ from the major part of itself $J^+(\mathbf{r})$ together with electric field $E^i(\mathbf{r}) + G_D(J^+)$. The output contrast current $J(\mathbf{r})$ is further processed to generate the contrast by $\chi(\mathbf{r}) = J(\mathbf{r}) / [E^i(\mathbf{r}) + G_D(J)]$. Inspired by the effects of basis-expansion on decreasing the difficulties in solving ISPs, it defines a combined loss function in a cascaded end-to-end (CEE) network with multiple labels to guide the learning process gradually and to decrease the nonlinearities of ISPs. Finally, inspired by the SOM, where the minor part of the induced current is chosen as unknowns, skip connections are added to link some specific layers so that the network is able to focus on the learning of minor part of induced current $J(\mathbf{r}) - J^+(\mathbf{r})$. The ICLM has made good use of $E^i(\mathbf{r})$, G_S , and G_D to a deeper degree and outperforms the DCS proposed in [18].

A time-domain acoustic wave ISP is solved in [33], which develops a theory-designed RNN. It finds that training such a network and updating its weights amount to a solution of the ISP and the process is equivalent to a gradient-based full-waveform inversion. The trainable weights in the RNN are chosen to be velocity parameters, which can be considered as acoustic counterpart of $1/\sqrt{\epsilon_r}$, up to a constant factor.

A summary of papers that solve inverse scattering problems using deep learning schemes is provided in Fig. 2.

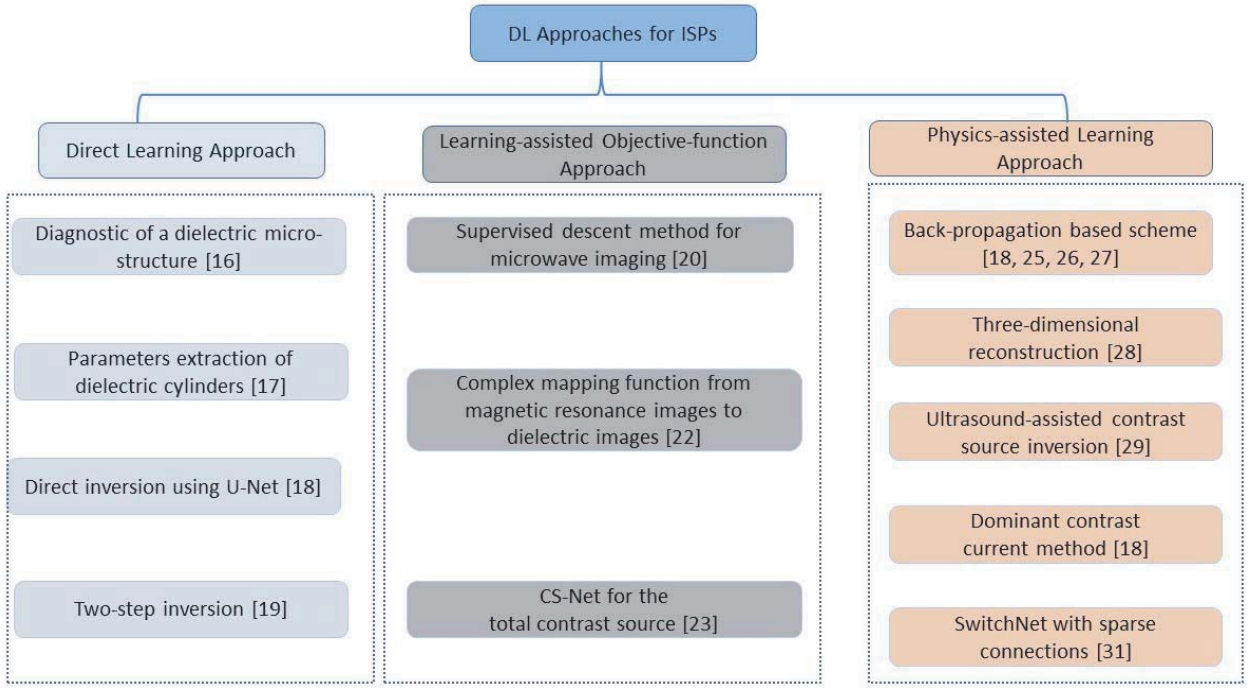


Figure 2. A summary of papers that solve inverse scattering problems using deep learning schemes. Note that [32] and [33] that belong to “other approaches” are not listed in the figure.

5. RECONSTRUCTION EXAMPLES

We present some reconstruction results using DL in this section. We test the performances of the DIS, BPS, and DCS that are proposed in [18]. The U-Net architecture, shown in Fig. 3, is adopted that consists of a contracting path (left side) and an expansive path (right side). The contracting path is a down-sampling process, consisting of repeated applications of 3×3 convolutions, batch normalization (BN), and ReLU, then followed by a 2×2 max pooling operation. The expansive path is an up-sampling process, where a 3×3 upconvolution replaces the max pooling operation in contracting path. For DCS, the number of output channels N_{out} is equal to the number of incidences and the average of the outputs for all incidences is chosen as the final result.

The various parameters of ISP are as follows. The DOI is with the size of $2 \times 2 \text{ m}^2$ that is discretized into 64×64 pixels. There are 16 line sources and 32 line receivers uniformly distributed on a circle of radius 3 m, which operate at 400 MHz. Scattering data are synthetically generated from 500 different scatterers, among which 475 are used to train DL networks and 25 are used to test the trained networks.

The first example considers a set of cylinders with random relative permittivity, radius, number, and location. The number of randomly generated cylinders is between 1 and 3 and the radii are between 0.15 and 0.4 m. Overlapping between cylinders is allowed so that the scatterers present sufficient complexity. The relative permittivity is set between 1 and 1.5. Scattered data are contaminated with 5% Gaussian noise. Fig. 4 presents reconstructed relative permittivity profiles of four representative tests, where we see that DIS can reconstruct only very simple profiles and the reconstructed profiles do not present sharp boundaries. In comparison, both BPS and DCS obtain satisfying results for all test cases. The reconstruction results obtained by different DL schemes can be quantitatively evaluated by the relative error that accounts for the normalized overall mismatch in all pixels. In this example, the relative error of DIS, BPS, and DCS is 5.8%, 1.7%, and 1.8%, respectively.

In the second example, the scatterers are modeled by the MNIST database, which is a widely used database of handwriting digits. We aim to quantitatively reconstruct the profile where the scatterers are represented by the digits. As shown in the first row of Fig. 5, some representative scatterers are

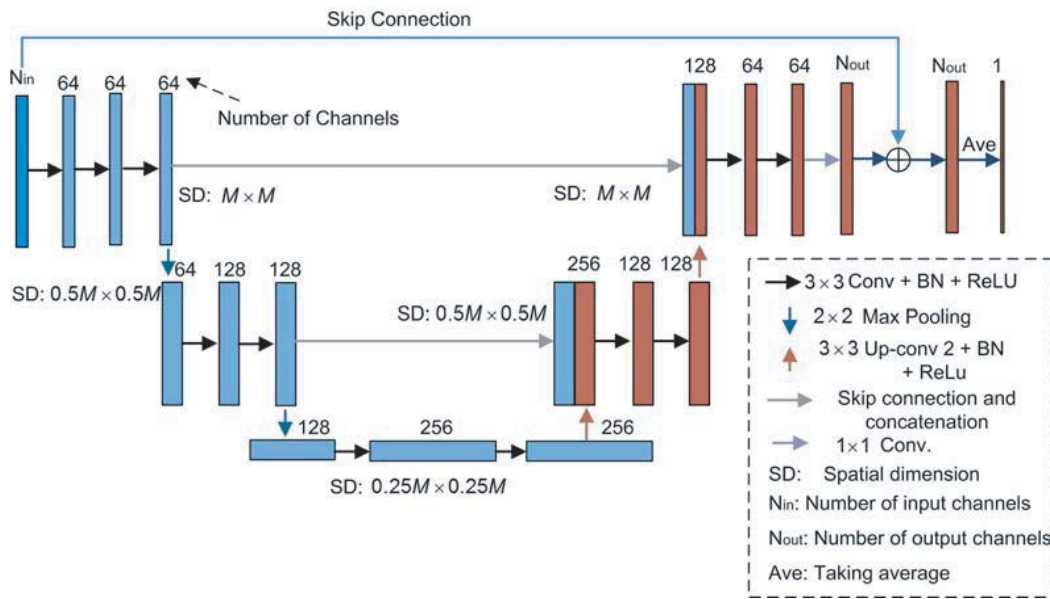


Figure 3. The U-Net architecture is adopted to test the performance of three ISP DL schemes: DIS, BPS, and DCS. (Reproduced with permission from [18]).

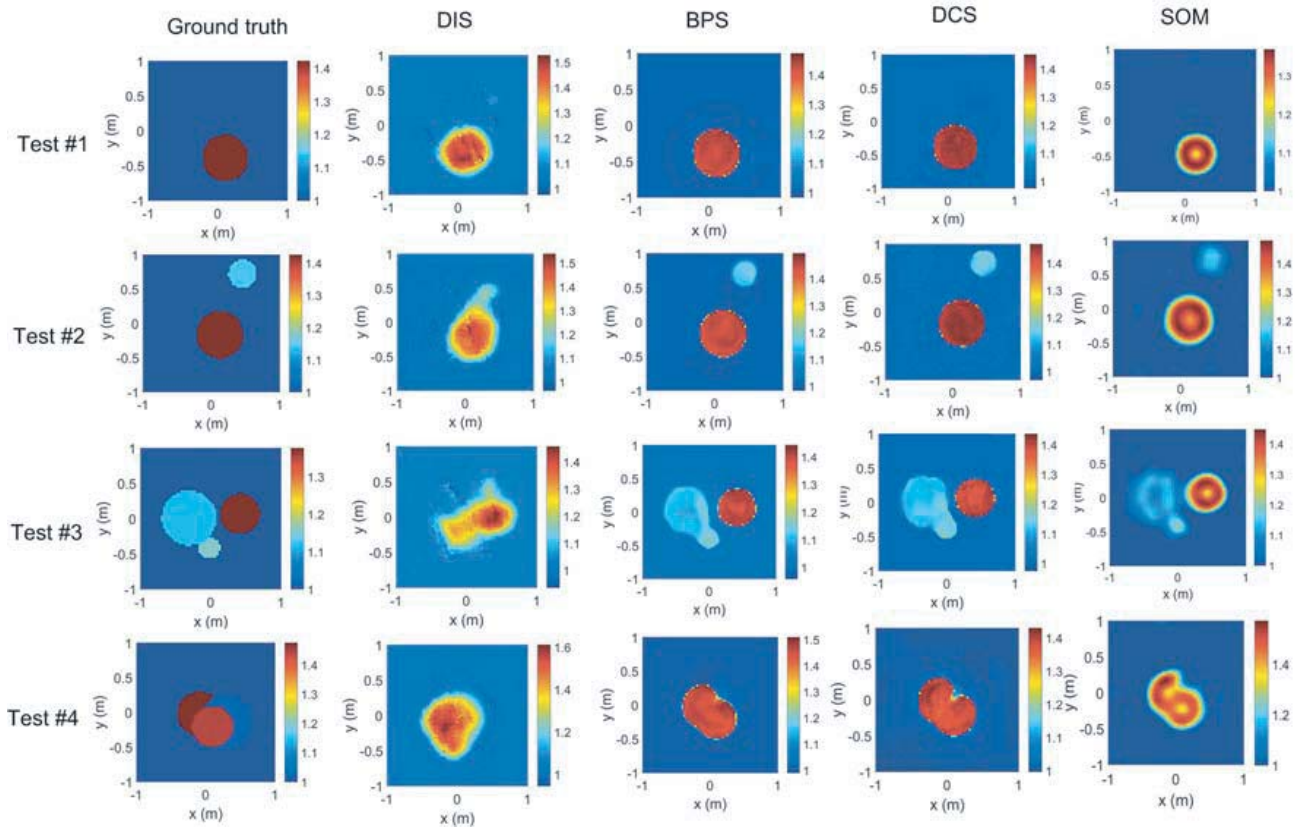


Figure 4. Reconstructed results for the case of random cylinders. The columns from the left are the ground-truth images and reconstructed images by the DIS, BPS, DCS DL schemes and an iterative method (SOM) for four representative profiles. (Reproduced with permission from [18]).

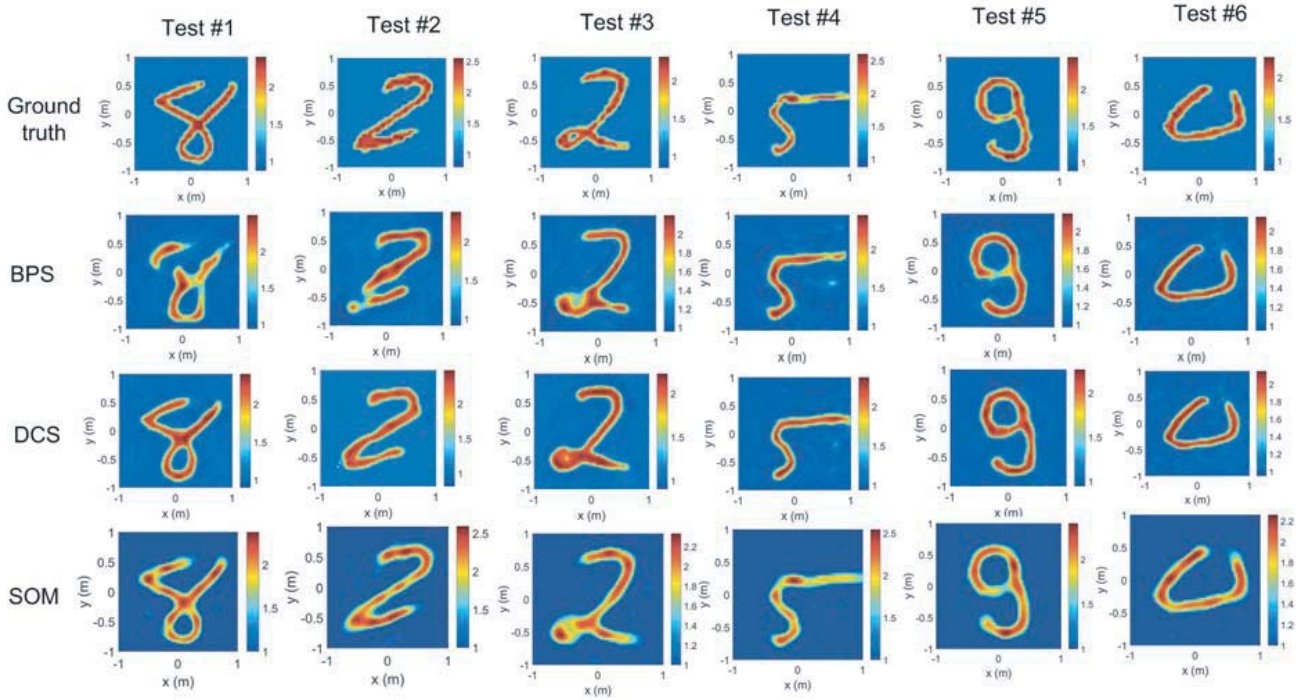


Figure 5. Reconstructed results for the case of MNIST database. The rows from the top are the ground-truth images and reconstructed images by the BPS, DCS, and SOM for six representative profiles. (Reproduced with permission from [18]).

set to be dielectric with a random relative permittivities between 2 and 2.5. The DIS fails for these complex scatterers, and thus the results are excluded from Fig. 5. We see that both BPS and DCS are able to reconstruct the profiles with satisfying results, but DCS seems to slightly outperform BPS. The relative error of BPS and DCS is 11.4% and 9.7%, respectively.

To test the generalization ability of trained DL network, we use the network trained with circular cylinders (in the first example) to test the MNIST profiles (in the second example), noting the differences between the two sets in terms of both the shapes and ranges of relative permittivities. The reconstructed results, displayed in Fig. 6, show that in spite of the degradation compared with the results obtained in the second example, BPS and DCS are still able to provide qualitatively satisfying results, i.e., the size, shape, and position of scatterers generally agree with the ground truth.

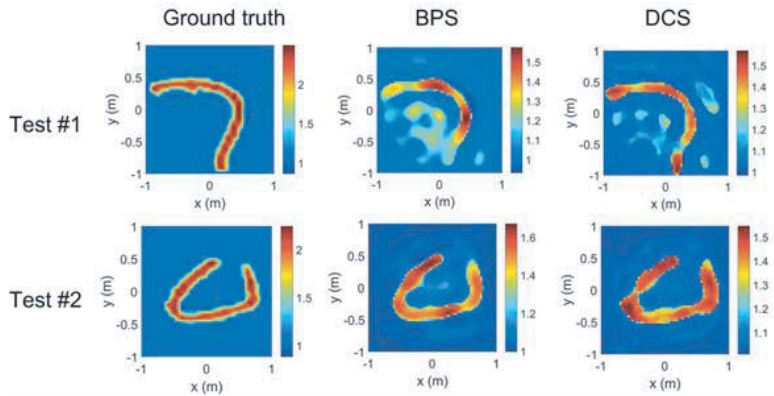


Figure 6. A test for generalization, where the network trained with circular cylinders is used to test the MNIST database. (Reproduced with permission from [18]).

We also test the performance of BPS and DCS using the experimental data measured at Institute Fresnel. For the two-circle scatterer depicted in Fig. 7, the reconstructed relative permittivity profiles from BPS and DCS at both 3 and 4 GHz are shown in Fig. 8, which shows that DCS has a better performance compared with BPS.

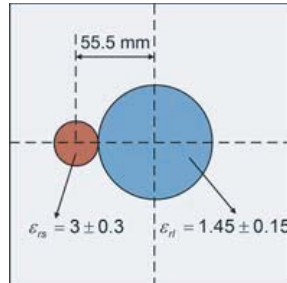


Figure 7. The ground-truth profile of “FoamDielExt” for experimental verification. The details of experimental setup can be found in [18] and references therein. (Reproduced with permission from [18]).

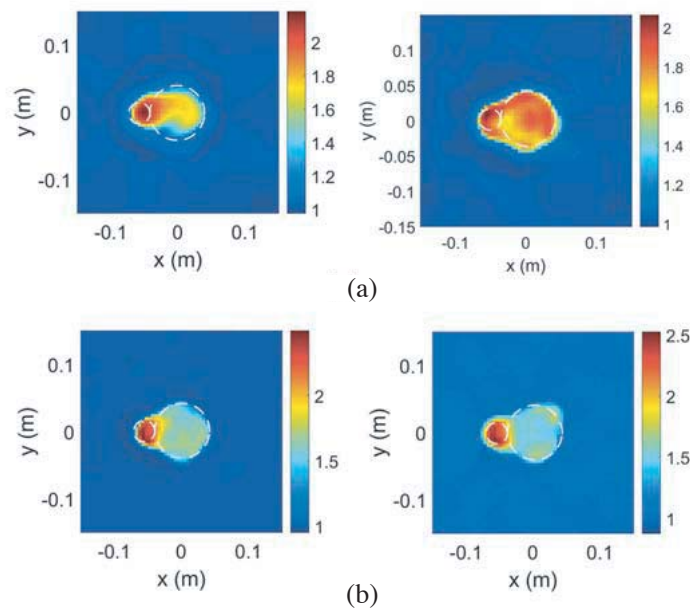


Figure 8. Reconstructed results of the “FoamDielExt” profile for (a) BPS and (b) DCS at (left) 3 GHz and (right) 4 GHz. (Reproduced with permission from [18]).

In all aforementioned results, we used a personal computer with CPU (3.4-GHz Intel Core i7 Processor and 16-GB RAM) and the running time is less than one second for testing. The time spent on both training and testing can be significantly reduced by GPU calculation.

6. DISCUSSIONS AND CONCLUSIONS

ISPs have been already an active research topic for a long time before DL emerges as a powerful technology. Over several decades, researchers have gained much insightful domain knowledge that has been leveraged on to devise approximate direct inversion models or effective iterative solvers. Thus, we should avoid using DL as a purely data-driven black-box solver, otherwise NNs have to spend unnecessary cost to train and learn well-know underlying wave physics. We should extract out as much as possible what we ourself can do by leveraging insightful domain knowledge and leave the remaining

to NN. For researchers in electrical engineering, existing NN architectures are often directly adopted to solve ISPs. In this case, it is crucial to design the input and output of NNs since the mathematical property of the mapping function from the input to output determines whether we pass a difficult or easy task to NNs. Roughly speaking, if the output depends in a much less nonlinear way on the input, then the learning task for NNs will be easier. It is important to stress that designing effective inputs and outputs of NNs needs a fairly good understanding of the corresponding forward problem. Many research efforts have been made in these directions in order to solve ISPs efficiently in terms of speed, accuracy, and robustness, i.e., achieving real-time high-quality quantitative imaging.

Despite the preliminary successes in solving ISPs, DL also poses its own challenges and limitations. We will discuss these fundamental questions and suggest possible future research directions and countermeasures.

6.1. Limitations

While NNs have been revolutionary tools for solving many tasks in computer vision or language processing, they have not provided a radical improvement, in terms of accuracy and robustness, over traditional non-learning methods for solving ISPs.

Since the DL approach is data-driven, instead of laying on any first principles, what is the confidence level of the results? As shown in Eq. (6), the loss function of NNs directly depends on the size and the variety of training data. It is now generally empirical, at least in the ISP community, to determine whether the size of training data is large enough and whether the variety of data is good enough to randomly sample the whole space \mathcal{X} of the solution x . If the size and the variety of training data is insufficient, then DL approach hardly works, regardless of what mathematical skills are used. In other words, a lack of information cannot be remedied by mathematical calculations. A common strategy to increase the training set size is data augmentation, where new (input, output) pairs are generated by transforming existing ones [9]. Nevertheless, a sufficiently complete exploit of the solution space is also a challenge in both theory and practice, especially for problems with a large number of parameters to reconstruct. Even if when the size and the variety of training data is sufficient, the design of NN architecture has to deal with two conflicting requirements [34]. The first is that the parametric model should be universal enough for a faithful representation of a large class of functions, i.e., to cover the whole space \mathcal{X} of the solution. The second is that the model should have a small number of parameters, i.e., expecting a decrease in computational complexity and an increase in robustness.

The quality of the trained NNs is typically measured by its ability to generalize from a training set to previously unseen data drawn from the same distribution as the one used for training. This ability is referred to as generalization. For ISPs, the training of NNs in fact amounts to learning the laws of scattering. Once the laws of scattering are sufficiently learnt from the training data set, then the trained NN is naturally able to work for unseen data. Consequently, the generalization ability of NNs for ISPs can be understood as how well the laws of scattering are learnt from the training data. A concept closely related to generalization is overfitting, which is a serious risk when NNs have a large amount of tuning parameters. In addition to the regularization technique presented in Eq. (6), a common strategy is to split the training data into a set used for fitting and another set used for validation. During training, which is an iterative process, the performance of NNs on the validation set is monitored, and training is terminated when the performance on the validation set begins to decrease [9]. In solving ISPs, regularization can also be implemented from physical perspectives. For example, [18] and [32] have applied truncated singular value decomposition (SVD) to generate physically meaningful input of NNs.

Compared with the learning approach, the classical objective-function approach relies exclusively on first principles and inherently produces outputs that are consistent with their inputs [35]. In addition, there is no concern about the generalization since the classical objective-function approach works for any valid measurement. The solution to the problem is indeed somewhere in the space \mathcal{X} of the model parameter x , but it is just difficult and time-consuming to find it out. Thus, from this viewpoint, the learning-assisted objective-function approach presented in Section 4.2 might be a better choice for integrating the two approaches, in terms of the level of confidence, accuracy, and robustness of the results. The speed of objective-function approach can be accelerated by learning approaches as an assistance.

6.2. Future Works

On the one hand, the insights that researchers have gained in developing approximate direct inverses or effective iterative solvers should be further exploited to improve the performance of NNs. For example, some iterative algorithms, such as the contraction integral equations [36, 37], are specially designed to tackle highly nonlinear ISPs, i.e., the case of strong scattering scatterer. A future direction would be incorporating the physical and mathematical insights presented in these algorithms into the architectures of NNs so as to reduce the degree of nonlinearity of the mapping function from the input to the output of NNs.

On the other hand, the state-of-the-art techniques developed in the DL community should also be referenced for tackling general regression problems, including ISPs. For example, the generative adversarial network (GAN) may offer a way to break current limits in supervised learning [7]. GANs are generative models since they create new data instances that resemble the training data. GANs consist of a generator NN that learns to produce the target output and a discriminator NN that learns to distinguish ground-truth data from the output of the generator. GANs are promising since they not only solve inverse problems, but also improve generalization capabilities.

The research work that applies NNs to solve other physics-based inverse problems might benefit the research of ISPs, and vice versa. For example, the problem of electric impedance tomography (EIT) exhibits great similarity to ISPs since the former is a quasi-static approximation of the latter. The Deep D-Bar approach [38], the dominant-current deep learning scheme (DC-DLS) [39], and the induced-current learning method (ICLM) [40] have been proposed for the realtime electrical impedance tomography of the chest. In [41], a dynamical touch sensing is studied by means of a spatio-temporal based EIT imaging on a conductive fabric. Photoacoustic tomography (PAT) is an imaging technique that utilizes coupled physics, i.e., acoustics and optics, both of which are governed by wave equations. In [42], a model-based learning NN has been tested on a set of segmented vessels from lung computed tomography scans and then applied to in-vivo photoacoustic measurement data. Indeed, many research societies are developing various DL models to achieve real-time quantitative imaging.

An inverse problem solver is closely related to its corresponding forward problem solver. The DL networks developed for solving the forward problem might bring some insights into solving the inverse problem. In [43], a DL technique is used to solve to a 2D electrostatic problem with significantly reduced computational time. Another promising research direction in the area of DL approaches for ISPs is to solve solve 3D inverse problems, since most real-world ISPs are 3D ones. A substantial increase in the number of model parameters, compared with its 2D counterpart, poses compelling challenges to DL networks. Only when DL approaches work well for 3D ISPs in real time, can we say DL approaches radically changed the way of solving ISPs. A preliminary research working on 3D case is [28], where a 3D electromagnetic ISP with layered media background is solved by using a 3D U-Net.

REFERENCES

1. Le Cun, Y., Y. Bengio, and G. Hinton, "Deep learning," *Nature*, Vol. 521, No. 7553, 436–444, 2015.
2. Li, H., Y. Yang, D. Chen, and Z. Lin, "Optimization algorithm inspired deep neural network structure design," *Proceedings of the 10th Asian Conference on Machine Learning*, (J. Zhu and I. Takeuchi, eds.), Vol. 95 of *Proceedings of Machine Learning Research*, 614–629, PMLR, Nov. 14–16, 2018.
3. Yang, Y., J. Sun, H. Li, and Z. Xu, "Deep ADMM-Net for compressive sensing MRI," *Advances in Neural Information Processing Systems*, Vol. 29, 10–18, Curran Associates, Inc., 2016.
4. Lu, Y., A. Zhong, Q. Li, and B. Dong, "Beyond finite layer neural networks: Bridging deep architectures and numerical differential equations," *International Conference on Machine Learning*, 3276–3285, 2018.
5. E, W., "A proposal on machine learning via dynamical systems," *Communications in Mathematics and Statistics*, Vol. 5, No. 1, 1–11, 2017.
6. E, W., J. Han, and Q. Li, "A mean-field optimal control formulation of deep learning," *Research in the Mathematical Sciences*, Vol. 6, No. 1, 10, 2019.
7. Goodfellow, I., Y. Bengio, and A. Courville, *Deep Learning*, MIT Press, 2016.

8. Chen, X., *Computational Methods for Electromagnetic Inverse Scattering*, Wiley, 2018.
9. McCann, M. T., K. H. Jin, and M. Unser, “Convolutional neural networks for inverse problems in imaging: A review,” *IEEE Signal Processing Magazine*, Vol. 34, No. 6, 85–95, 2017.
10. Lucas, A., M. Iliadis, R. Molina, and A. K. Katsaggelos, “Using deep neural networks for inverse problems in imaging: beyond analytical methods,” *IEEE Signal Processing Magazine*, Vol. 35, No. 1, 20–36, 2018.
11. Massa, A., D. Marcantonio, X. Chen, M. Li, and M. Salucci, “DNNs as applied to electromagnetics, antennas, and propagation — A Review,” *IEEE Antennas and Wireless Propagation Letters*, Vol. 18, No. 11, 2225–2229, 2019.
12. Caorsi, S. and P. Gamba, “Electromagnetic detection of dielectric cylinders by a neural network approach,” *IEEE Transactions on Geoscience and Remote Sensing*, Vol. 37, No. 2, 820–827, 1999.
13. Rekanos, I. T., “Neural-network-based inverse-scattering technique for online microwave medical imaging,” *IEEE Transactions on Magnetics*, Vol. 38, 1061–1064, Mar. 2002.
14. Bermani, E., A. Boni, S. Caorsi, and A. Massa, “An innovative real-time technique for buried object detection,” *IEEE Transactions on Geoscience and Remote Sensing*, Vol. 41, 927–931, Apr. 2003.
15. Salucci, M., N. Anselmi, G. Oliveri, P. Calmon, R. Miorelli, C. Reboud, and A. Massa, “Real-time NDT-NDE through an innovative adaptive partial least squares SVR inversion approach,” *IEEE Transactions on Geoscience and Remote Sensing*, Vol. 54, No. 11, 6818–6832, 2016.
16. Ran, P., Y. Qin, and D. Lesselier, “Electromagnetic imaging of a dielectric micro-structure via convolutional neural networks,” *2019 27th European Signal Processing Conference (EUSIPCO)*, 1–5, IEEE, 2019.
17. Fajardo, J., J. Galvn, F. Vericat, M. Carlevaro, and R. Irastorza, “Phaseless microwave imaging of dielectric cylinders: An artificial neural networks-based approach,” *Progress In Electromagnetics Research*, Vol. 166, 95–105, Dec. 2019.
18. Wei, Z. and X. Chen, “Deep-learning schemes for full-wave nonlinear inverse scattering problems,” *IEEE Transactions on Geoscience and Remote Sensing*, Vol. 57, No. 4, 1849–1860, 2019.
19. Yao, H. M., W. E. I. Sha, and L. Jiang, “Two-step enhanced deep learning approach for electromagnetic inverse scattering problems,” *IEEE Antennas and Wireless Propagation Letters*, Vol. 18, No. 11, 2254–2258, 2019.
20. Guo, R., X. Song, M. Li, F. Yang, S. Xu, and A. Abubakar, “Supervised descent learning technique for 2-D microwave imaging,” *IEEE Transactions on Antennas and Propagation*, Vol. 67, No. 5, 3550–3554, 2019.
21. Adler, J. and O. Öktem, “Solving ill-posed inverse problems using iterative deep neural networks,” *Inverse Problems*, Vol. 33, No. 12, 124007, 2017.
22. Chen, G., P. Shah, J. Stang, and M. Moghaddam, “Learning-assisted multi-modality dielectric imaging,” *IEEE Transactions on Antennas and Propagation*, 1–14, 2019.
23. Sanghvi, Y., Y. Kalepu, and U. K. Khankhoje, “Embedding deep learning in inverse scattering problems,” *IEEE Transactions on Computational Imaging*, Vol. 6, 46–56, 2020.
24. Chen, X., “Subspace-based optimization method for solving inverse scattering problems,” *IEEE Trans. Geosci. Remote Sens.*, Vol. 48, 42–49, 2010.
25. Sun, Y., Z. Xia, and U. S. Kamilov, “Efficient and accurate inversion of multiple scattering with deep learning,” *Optics Express*, Vol. 26, No. 11, 14678–14688, 2018.
26. Li, L., L. G. Wang, F. L. Teixeira, C. Liu, A. Nehorai, and T. J. Cui, “DeepNIS: Deep neural network for nonlinear electromagnetic inverse scattering,” *IEEE Transactions on Antennas and Propagation*, Vol. 67, No. 3, 1819–1825, 2019.
27. Li, L., L. G. Wang, and F. L. Teixeira, “Performance analysis and dynamic evolution of deep convolutional neural network for electromagnetic inverse scattering,” *IEEE Antennas and Wireless Propagation Letters*, Vol. 18, No. 11, 2259–2263, 2019.
28. Xiao, J., J. Li, Y. Chen, F. Han, and Q. H. Liu, “Fast electromagnetic inversion of inhomogeneous scatterers embedded in layered media by born approximation and 3-D U-Net,” *IEEE Geoscience and Remote Sensing Letters*, 1–5, 2019.

29. Khoshdel, V., A. Ashraf, and J. LoVetri, "Enhancement of multimodal microwave-ultrasound breast imaging using a deep-learning technique," *Sensors*, Vol. 19, No. 18, 4050, 2019.
30. Van den Berg, P. M. and R. E. Kleinman, "A contrast source inversion method," *Inverse Probl.*, Vol. 13, 1607–1620, 1997.
31. Khoo, Y. and L. Ying, "SwitchNet: a neural network model for forward and inverse scattering problems," *SIAM Journal on Scientific Computing*, Vol. 41, No. 5, A3182–A3201, 2019.
32. Wei, Z. and X. Chen, "Physics-inspired convolutional neural network for solving full-wave inverse scattering problems," *IEEE Transactions on Antennas and Propagation*, Vol. 67, No. 9, 6138–6148, 2019.
33. Sun, J., Z. Niu, K. A. Innanen, J. Li, and D. O. Trad, "A theory-guided deep-learning formulation and optimization of seismic waveform inversion," *Geophysics*, Vol. 85, No. 2, R87–R99, 2020.
34. Unser, M., "A representer theorem for deep neural networks," *Journal of Machine Learning Research*, Vol. 20, No. 110, 1–30, 2019.
35. Belthangady, C. and L. A. Royer, "Applications, promises, and pitfalls of deep learning for fluorescence image reconstruction," *Nature Methods*, 1–11, 2019.
36. Zhong, Y., M. Lambert, D. Lesselier, and X. Chen, "A new integral equation method to solve highly nonlinear inverse scattering problems," *IEEE Transactions on Antennas and Propagation*, Vol. 64, No. 5, 1788–1799, 2016.
37. Zhong, Y., M. Salucci, K. Xu, A. Polo, and A. Massa, "A multiresolution contraction integral equation method for solving highly nonlinear inverse scattering problems," *IEEE Transactions on Microwave Theory and Techniques*, 1–14, 2019.
38. Hamilton, S. J. and A. Hauptmann, "Deep D-Bar: Real-time electrical impedance tomography imaging with deep neural networks," *IEEE Transactions on Medical Imaging*, Vol. 37, 2367–2377, Oct. 2018.
39. Wei, Z., D. Liu, and X. Chen, "Dominant-current deep learning scheme for electrical impedance tomography," *IEEE Transactions on Biomedical Engineering*, Vol. 66, No. 9, 2546–2555, 2019.
40. Wei, Z. and X. Chen, "Induced-current learning method for nonlinear reconstructions in electrical impedance tomography," *IEEE Transactions on Medical Imaging*, 1–9, 2019.
41. Duan, X., S. Taurand, and M. Soleimani, "Artificial skin through super-sensing method and electrical impedance data from conductive fabric with aid of deep learning," *Scientific Reports*, Vol. 9, No. 1, 8831, 2019.
42. Hauptmann, A., F. Lucka, M. Betcke, N. Huynh, J. Adler, B. Cox, P. Beard, S. Ourselin, and S. Arridge, "Model-based learning for accelerated, limited-view 3-D photoacoustic tomography," *IEEE Transactions on Medical Imaging*, Vol. 37, 1382–1393, Jun. 2018.
43. Tang, W., T. Shan, X. Dang, M. Li, F. Yang, S. Xu, and J. Wu, "Study on a Poisson's equation solver based on deep learning technique," *2017 IEEE Electrical Design of Advanced Packaging and Systems Symposium (EDAPS)*, 1–3, Dec. 2017.